OPTOELECTRONICS AND ADVANCED MATERIALS – RAPID COMMUNICATIONS Vol. 3, No. 9, September 2009, p. 884 - 890

Characterization of the ZnO thin films obtained by chemical route

S. MIHAIU*, M. GARTNER, M.VOICESCU, M. GABOR[a], O. MOCIOIU, M. ZAHARESCU
"Ilie Murgulescu" Institute of Physical Chemistry of the Romanian Academy, Spl. Independentei 202, 060021 Bucharest, Romania
[a]Tehnical University of Cluj-Napoca, Materials Science Laboratory-Thin Films, George Baritiu 26-28, 400027 Cluj – Napoca, Romania

Zinc oxide is classically known for its semiconducting and piezoelectric properties and its use in Schottky diodes and light emitting devices. Its wide direct energy band gap and large excitation binding energy continues to make it an attractive material for nanodevice applications including field effect transistors and bio-molecular sensors.
This work presents the characteristics of ZnO films obtained by chemical route, deposited by dip coating on the silicon and glass substrates. The resulting films consolidated by thermal treatment for one hour at 500 ˚C are slightly crystallized. IR-spectra show the characteristics bands of zinc oxide in the 440-490 cm^{-1} range. Refractive index and extinction coefficients calculated from SE data indicate that thin porous films are obtained. The studied films show a fluorescence emission at room temperature in the UV spectral region. Electrical resistance measurements of the films were performed in the 300-600˚C temperature range.

(Received July 31, 2009; accepted September 15, 2009)

Keywords: ZnO films, chemical route, optical properties, electrical behaviour

1. Introduction

Zinc oxide due to its semiconducting and piezoelectric properties, a wide direct energy band gap and large excitation binding energy continues to be an attractive material for nanodevice applications in information technologies (IT), biotechnology (BT) and environmental technology (ET). Undoped and doped zinc oxide films have been widely used as photoanode of solar cells [1-3], gas sensors [4-6], biosensors [7-9] varistors [10], film bulk acoustic resonators (FBAR) [11] transparent conductive oxide (TCO) for energy efficient windows [12].

Zinc oxide based films have been deposited on various substrates by sputtering with different forms [13-14], pulsed laser [15-16], chemical bath deposition [16], spray pyrolysis method [18-19], chemical vapour deposition [12], vapour transport deposition [20] and sol-gel process [4,21-23].

Zinc acetate dihydrate is usually used as a reagent for obtaining zinc oxide films by chemical route. In this compound zinc is octahedral coordinated, wherein both acetate groups are bidentate. The structural formula units are firmly linked by strong hydrogen bonds to form two-dimensional sheets; only week Van der Waals forces exist between such sheets. This sheet like nature of the structure accounts for such physical properties, as the mosaic character, softness and ready cleavage of the crystals [8]. Zinc acetate dihydrate, 2-methoxyethanol and monoethanolamine were used as starting materials by Hsieh at al [20] for obtaining ZnO thin films by sol-gel technology. Schuler and Aegerter [22] obtained ZnO:Al multilayer coatings with low electrical resistivity and good optical properties by sol-gel process. They started with zinc acetate dihydrate, isopropanol as solvent, and diethanolamine (DEA) as chelating agent. Hu at al [8] mention that well aligned ZnO nanorods have been fabricated on polyethylene terephthalate (PET) and FTO substrates by chemical bath deposition using ZnO seeds derived from a methanol solution of zinc acetate dihydrate and NaOH, kept for 2 h at low temperature of 60˚C.

In the present work we proposed the structural, morphological, optical and electrical characterization of the ZnO films obtained by chemical route using zinc acetate dihydrate as zinc precursor, ethanol as solvent and triethanolamine-TEA as chelating agent (molar ratio of precursor/TEA=5/1).

2. Experimental

2.1. Obtaining of the films

The experimental conditions used for preparing the solutions needed for films deposition were established on the previous paper published by Shuler and Aegerter [22]. In our work the diethanolamine was replaced by triethanolamine which allowed a significant reduction in the amount of the required chelating agent used in order to obtain stable solutions of precursors (TEA/Zn = 1/5, as compared to DEA/Zn = 1/1).

Zinc oxide sols of 0.1 M were obtained by dissolving of zinc acetate dihydrate (ZAD) into absolute ethyl alcohol (Riedel-deHaen) and triethanolamine (TEA) (Baker Analyzed) as catalyst and chelating agent. All reagents

used in the synthesis were p.a. grade. Zinc acetate dihydrate was stirred in absolute ethanol at 50˚C for 15 minutes, then triehanolamine in a molar ratio of ZAD/TEA=5/1 was slowly added drop wise and was continued with stirring at the same temperature for two hours for the obtaining of Zn-solution. The clear and homogenous solution was stored for 24 hours before using for film deposition. ZnO films were deposited by dip-coating on a carefully cleaned soda-lime-silica substrate and on thermally oxidized silicon wafers.

The consolidation of the films on the substrates was performed by thermal treatment at 500˚C for 5 min with a heating rate of 5°C/min according to the results of DTA and TG/DTG analysis presented in section 3.1. For multilayer coatings after each deposition the same thermal treatment was applied. All samples were additionally annealed at 500˚C for 1 hour. The experimental conditions of the films deposition and densification were previously presented in the paper [24].

The unconsolidated film was labelled ZnO-F_{unc} and the consolidated films obtained by multilayer depositions were abbreviated as ZnO-F_n where n=1,2,3,4,5 corresponds to the number of the deposition.

2.2. ZnO films characterization

DTA and TG/DTG investigations were performed with a Mettler Derivatograph in the 20-1000 ˚C temperature range with a heating rate of 5˚C/min.

XRD analysis of the films was performed with Bruker D8 Advance diffractometer in the Bragg-Brentano configuration. The scanning was made at room temperature in the range of 5–90°, with steps of 0.01 and 4 °/second.

FT-IR spectroscopy measurements were realized with a Nicolet 6700 apparatus in 400–4000 cm^{-1} domain.

The AFM experiments were carried out in the dynamic (non-contact) mode using an EasyScan 2 apparatus (Nanosurf AG, Switzerland) by means of a 10 µm × 10 µm scanner with vertical range of 2 µm and z-axis resolution of 0.027 nm. The scan rate was in the range of 1–2 Hz. The cantilever was with spring constants of about 34 N/m and the shape of the SiN tips was square pyramidal with radius of curvature of less than 10 nm and half angle 350. Scanning Probe Image Processor (SPIP™) software package (version 4.6.0.0) was used for image processing in terms of roughness and grain analysis.

The thickness of the layers (*d*) was calculated from Spectroellipsometric data obtained with a null type ellipsometer. Experimental SE spectra have been simulated using the multilayer and multicomponent Bruggemann's Effective Medium Approximation (BEMA) model [25].

The fluorescence spectra (emission and excitation) were recorded with Perkin Elmer 204 spectrofluorimeter (having a Xe lamp of 150 W), interfaced to a computer, permitting a prestabilized reading time of the data. Usually the time range between two measurements is 550 ms.

Electrical resistance measurements were performed by "the four point method".

In order to obtain low specific resistance Ohmic contacts on the film surface [26], Ti(20nm)/Au(30nm) ohmic electrodes were deposited, ex-situ, on the films surface by UHV e-beam evaporation. Copper leads were attached to the electrode with silver paste and were connected to an automatic polarization system. The electric voltage (V) was then measured with applied currents (I). The films were put in an atmosphere controlled tubular furnace and the heating rate was 5°C/min.

3. Results and discussion

The stable, clear and homogenous sol obtained by the procedure presented in section 2.1 was used for deposition by dip coating of the films on glass and silicon wafer.

3.1. Structural and thermal characterization of the dried gel

In Fig. 1 the FT-IR spectra of the dried gel and of the powder resulted after thermal treatment of the dried gel at 500˚C are presented.

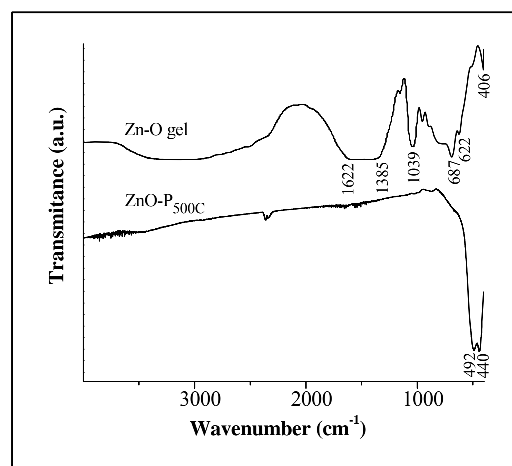

Fig. 1 FT-IR spectra of the dried gel and ZnO powder (obtained by thermal treatment of the dried gel at 500^0 C for 1hour).

The dried-gel presents the characteristic bands of O-H stretching at 3000-3500 cm^{-1} and of the adsorbed water in the 1600 cm^{-1} region; the carboxylate bands (asymmetric and symmetric stretching of C=O, respectively) at 1385 cm^{-1} and νC-C of organic salts at 1039 cm^{-1}. Based on FT-IR data one may assume that during the gelation process a Zn-hidroxo-acetate gel was obtained and triehanolamine has acted mainly as catalyst.

The DTA/TGA and DTG curves of the dried gel are shown in Fig.2. The first two endothermic effects at 76 and 133˚C, respectively, are assigned to the evolution of ethanol and water.

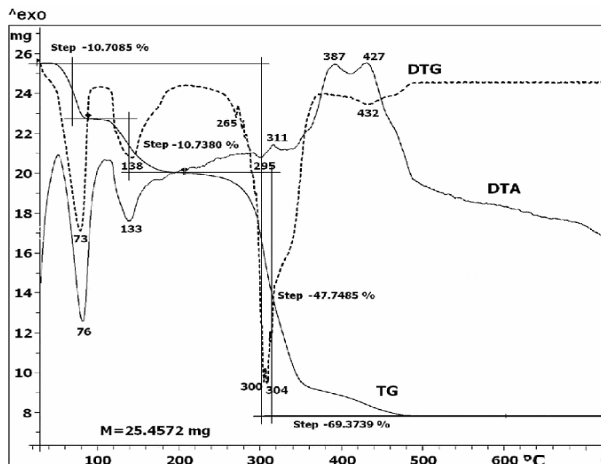

Fig. 2 DTA/ TG analysis of the ZnO – dried gel.

The decomposition of the Zn-hidroxo-acetate gel takes place simultaneously with the oxidation of the resulted CO to CO_2 at about 300^0C. The two reactions are accompanied by two small thermal effects, one at 295^0C (endothermic peak) assigned to decomposition of the gel and the other 311˚C (exothermic peak) assigned to CO oxidation. The low intensity of the peaks could be explained by the fact that a superposition and a compensation of the two phenomena take place. The corresponding weight loss is 47.7%. The exothermic peak at around 387 and 427 ˚C may be assigned to the combustion of organic component and crystallisation of ZnO from the studied gel. After 500˚C, the TG curve remains constant suggesting that a thermal treatment at this temperature could be used to obtain ZnO. The thermal analysis of the ZnO-dried gel indicates that the total elimination of the organic component occurs at the temperature with 80˚C higher than in the case of zinc acetate (427˚C for the gel and 347˚C for zinc acetate) suggesting the stronger stability of the gel network.

In the FT-IR spectrum of the ZnO powder obtained by thermal treatment at 500^0C all organic bands practically disappear and characteristic band of zinc oxide network appears in the 440-492 cm^{-1} spectral range indicating that the material consists of pure ZnO without carbon rests.

3.2 Structural and morphological characterization of the ZnO films

The as-prepared films both on the glass and silicon supports are amorphous and no characteristic peaks appear in the X-Ray diffraction patterns.

By thermal treatment at 500^0C the slight crystallization of ZnO was observed by the presence of the diffraction lines at (100) (002) (101) and (110) (data not presented here).

FT-IR spectra performed on the ZnO-F_{4T} films deposited on glass as well as on silicon wafer present only characteristic bands assigned to Zn-O bonding at 420 cm^{-1} and 440 cm^{-1}, respectively.

In the Fig. 3(a) and (b) the 2D and 3D - AFM images of the ZnO-F_{5T} films (after five layers deposition) deposited on glass support are presented. The surface roughness was determined as equal to 3.22 nm. The grain with the cocoon like appearance can be observed.

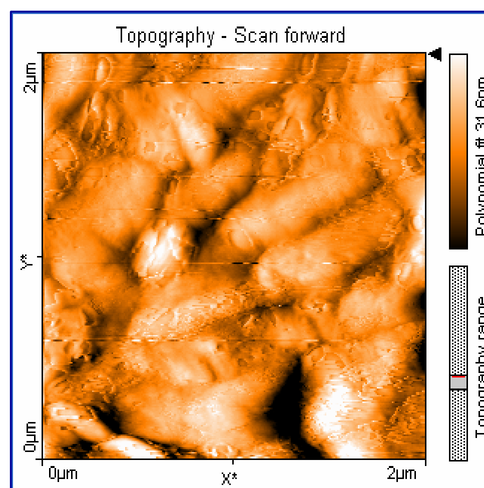

(a)

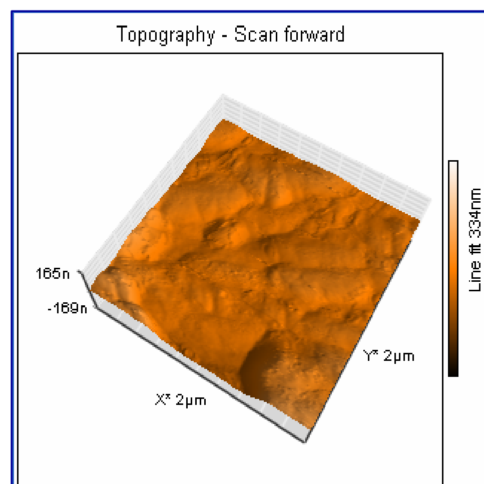

(b)

Fig. 3. AFM images of the ZnO-F_{5T} thermally treated films on glass: (a) 2D image; (b) 3D image (RMS = 3.22 nm).

Fig. 4 (a) and (b) displays the surface morphology of the ZnO-F_{5T} on silicon wafer

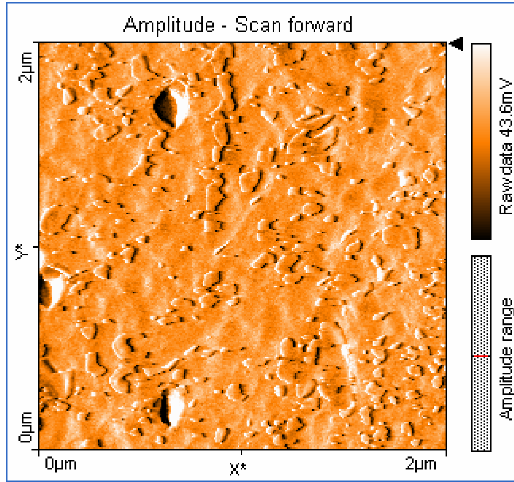

(a)

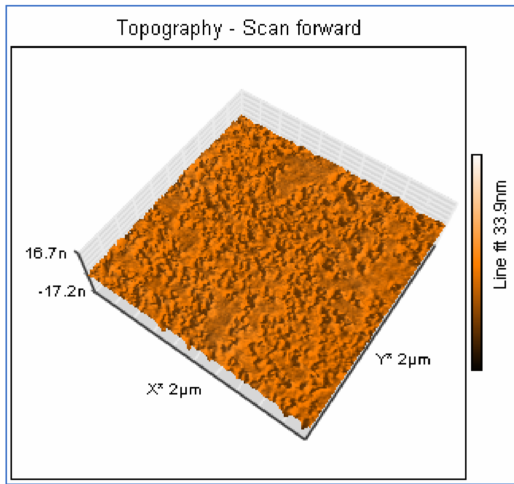

(b)

Fig. 4. AFM images of the ZnO-F5T thermally treated films on silicon wafer: (a) 2D image;(b) 3D image (RMS = 6.81 nm).

In this case the surface roughness characterized by the Root-Mean-Square (RMS) parameter has the value of 6.81 nm. It is evident that surface morphology strongly depends on the type of support.

3.3. Optical characterization of the ZnO films

Optical constants and structural characterization of the ZnO-based films was made using the spectroscopic ellipsometry (SE) method.

The thickness of the layers (d) obtained from the best fit [corresponding to the minimum of the error, calculated from equation (1)] is presented in Table 1,

$$Error = \sum_{i=1}^{N}\left[\left(R_i^{ec} - R_i^{em}\right)^2 + \left(I_i^{mc} - I_i^{me}\right)^2\right]/N, \qquad (1)$$

with: R_e - real part of ellipsometric function (tanPSI*cosDELTA),

R^{ec}_i - calculated value,

R^{em}_i - measured value,

I_m - imaginary part of ellipsometric function (tanPSI*sinDELTA),

I^{mc}_i - calculated value,

I^{me}_i - measured value,

N - number of experimental points.

Table 1. Thickness (D) of the ZnO films.

ZnO films on the glass			
Sample		D (nm)	ε *10^{-7}
ZnO-F_{unc}		182	2839
ZnO-F_{5T}		605	17256
ZnO films on the silicon			
Sample	Buffer	Film	
	D_{SiO2} (nm)	D (nm)	ε *10^{-7}
ZnO-F_{unc}	557	17	102241
ZnO-F_{5T}	557	34	239681

The thickness of the ZnO-F_{unc} (D = 182 nm) on the glass support is almost 10 times higher than the same parameter of the films deposited on silicon (D=17 nm) (see Table 1). The same behaviour can be observed for consolidated ZnO-F_{5T} films (five layers depositions). In literature it is mentioned that on SiO_x/Si substrate the thickness of the ZnO film obtained by aqueous sol-gel route does not exceed 20 nm, pointing out the weak adherence of the solution to the SiO_x/Si substrate [27].

Optical constants (refractive index and extinction coefficient) for films supported on glass are presented in Fig. 5 (a) and (b) and for similar films on silicon in Fig. 6 (a) and (b).

For as prepared films (ZnO-F_{unc}) the optical constants (refractive index with 1.50< n<1.55 values and extinction coefficient k<0.06) have similar values on both types of substrates. The values of the refractive index of 1.85-2.0 and, consequently, of the extinction coefficient of 0.01-0.33, comparable with literature data [21] were obtained only for the ZnO-F_{5T} films deposited on the glass substrate. This indicates an increase of the film density. The optical constants of the ZnO-F_{5T} film supported on silicon are smaller even than for the as prepared film (see Figs.5 and 6), probably, due to the high porosity of the sample.

The fluorescence emission spectra (λ_{ex} =270 nm) were performed at room temperature on the ZnO films, both on the glass support (Fig. 7 (a)) as well as on silicon wafer (Fig. 7 (b)).

The spectra of ZnO-F_{1T}, ZnO-F_{2T}, ZnO-F_{3T} and ZnO-F_{4T} films deposited on the glass substrate (Fig. 7 (a)) show a strong UV emission at ~388 nm, a blue-green band at ~460 nm and a green band at ~ 524 nm, being similar to those reported in literature [28]. The UV emission peak of ZnO thin film is assigned to the excitonic related

recombination. The blue-green emission could be assigned to transition from the top of the valence band to the interstitial zinc level and the green band emission corresponds to the singly ionized oxygen vacancy in ZnO.

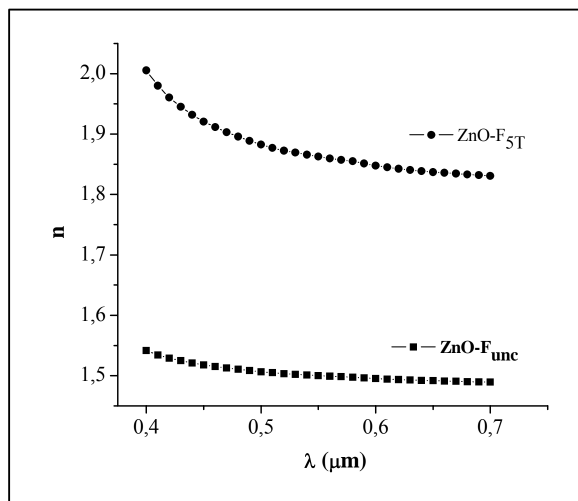

(a)

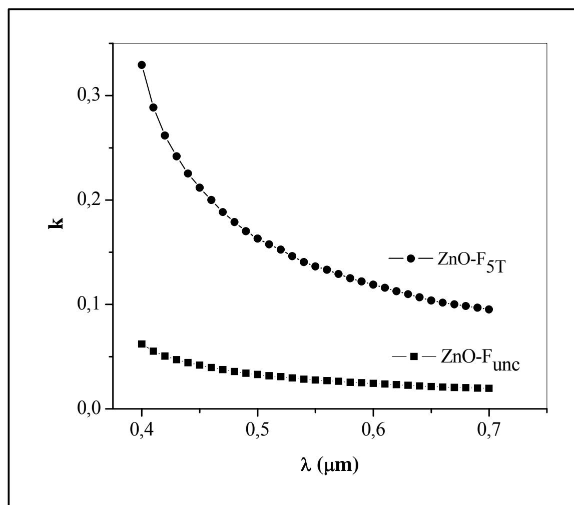

(b)

Fig. 5. Optical constants (n, k) of the ZnO –F_{unc} and ZnO-F_{5T} films: (a) refractive index (n;)(b) extinction coefficient (k).

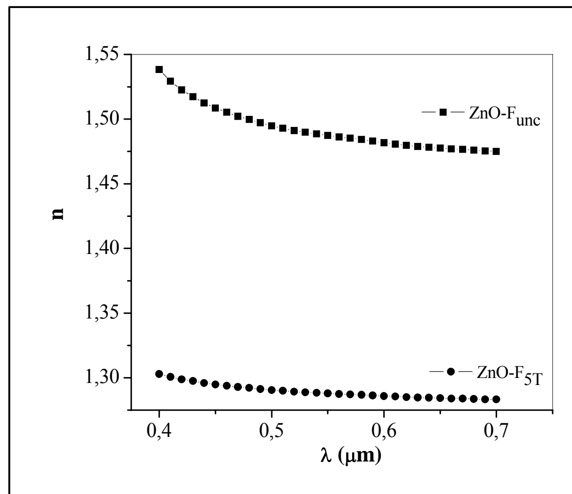

(a)

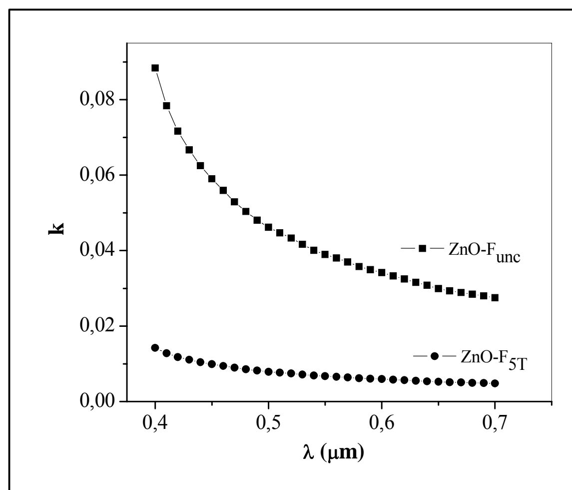

(b)

Fig. 6. Optical constants (n, k) of the ZnO-F_{unc} and ZnO-F_{5T} films: (a) refractive index (n); (b) extinction coefficient (k).

For the consolidated ZnO films on silicon (Fig. 7 (b)) two broad peaks in the 350-550 nm range are observed in the fluorescence emission spectra. The decrease in the emission bands intensity with the increase number of the deposition layers was revealed due to the growth of the grain size, probably.

3.4. Electrical properties

The resistance of the ZnO films was measured by a standard four-probe technique. The measurements were made very carefully and repeated five times to make sure that it is the true behaviour of the studied films.

Fig. 8 shows the temperature dependence of the electrical resistance of the ZnO-F_{5T} film on silicon wafer.

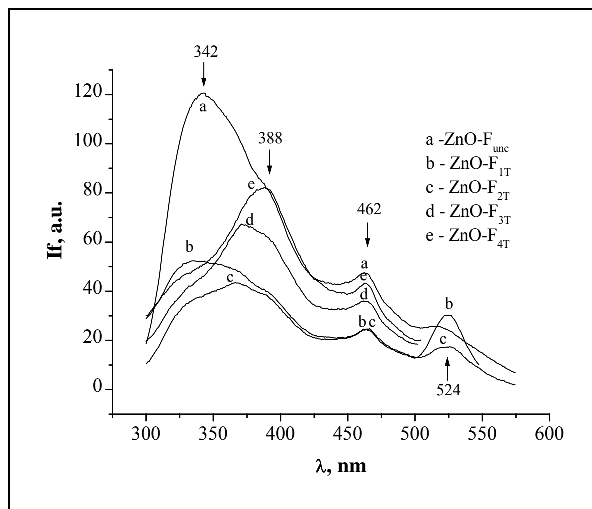

(a)

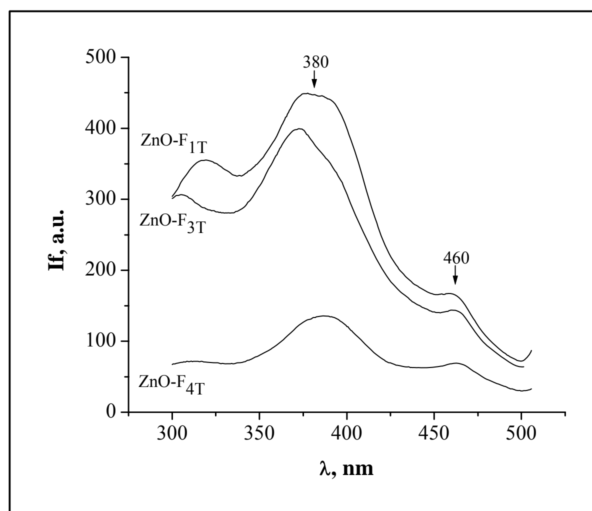

(b)

Fig. 7. Fluorescence spectra of the ZnO films:(a) on glass support; (b) on silicon support.

The resistance shows clear temperature dependence. For relative low temperatures (<100˚C) the gradual decrease in the resistance with increasing temperature can be accredited to the thermal excitation of electrons into the conduction band. For higher temperatures (>150˚C) it is probably to have a mix contribution: one due the thermal excitation of electrons into the conduction band and the other due to the O^{-1}_2 desorption. When the film temperature rises, the chemisorbed O^{-1}_2 is desorbed from the film surface, donating an electron to ZnO ($O^{-1}_2 \Rightarrow O_2$ +e), causing the resistance to decrease.

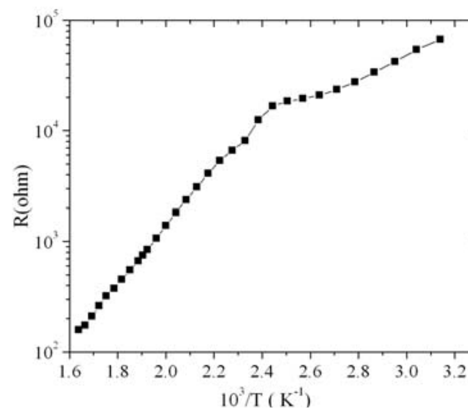

Fig. 8. Electrical resistance versus $10^3/T$ of the ZnO-F_{5T} film.

4. Conclusions

The thin ZnO films deposited by dip-coating technique on glass and silicon wafers were obtained by chemical route.

Morphology of the ZnO based films is strongly influenced by the substrates of the film.

More porous and thinner films with smaller refractive index were obtained on silicon wafers as compared with those deposited on the glass support.

All the studied films present the fluorescence emission in UV spectral range.

An n-type semiconducting behaviour in the 20-600 ˚C temperature range has been emphasized for the ZnO films deposited on the silicon wafer.

References

[1] M. Shaheer, M.Akhtara, M. Khana, M. S. Jeonb, O. B. Yanga, Electrochimica Acta **53**, 7869 (2008).
[2] A. Nemeth, Cs. Major, M. Fried, Z. Labadi, I. Barsony, Thin Solid Films **516,** 7016 (2008).
[3] C. Lin, H. Lin, J. Li, X. Li, J. Alloys and Compounds **462**, 175 (2008).
[4] G. S. Devi, V. B.Subrahmanvam, S. C.Gadkari, S. K. Gupta, Analytica Chimica Acta **568** (1-2), 41 (2006).
[5] E. Fortunato, A. Goncalves, A. Marques, A. Pimentel, P. Barquinha , H. Aguas, L. Pereira, L. Raniero, G. Goncalves, I. Ferreira, R. Martins, PTS 1and 2 Materials Science Forum **3-7**, 514 (2006).
[6] X. L. Cheng , H. Zhao, L. H. Huo, S. Gao, J. G. Zhao, Sensors and Actuators B-Chemical **102**(2), 248 (2004).
[7] C. F. Tang, S. A. Kumar, S. M. Chen, Analytical Biochemistry **380,** 174 (2008) .
[8] X .Hu, Y. Masuda, T. Ohji, K. Kato, J. Colloid and Interface Science **325**, 459 (2008) .

[9] A. Dorfman , N. Kumar, J.I.Hahm, Langmuir **22**(11), 4890 (2006).
[10] P. R. Bueno, J. A.Varela, E. Longo, J. Eur. Ceram. Soc. **28**, 505 (2008).
[11] R. C. Lin, Y. C. Chen, K. S. Kao, Appl. Phys. A **89**, 475 (2007).
[12] J. Hu., R. G.Gordon , J. Appl. Phys. **71**(2), 880 (1992).
[13] M. Bouderbala, S. Hamzaoui, B. Amrani, A. H. Reshak, H. M. Adnane, T. Sahraoui, M. Zerdali, Physica B **403,** 3326 (2008).
[14] S. H. Choi, J. S. Kim, Ultramicroscopy **108**, 1288 (2008).
[15] H. Yu, W. Zhang , Mat. Lett. **62,** 4263 (2008).
[16] T. Mazingue, L. Escoubas, L. Spalluto, F. Flory, G. Socol, C. Ristoscu, E. Axente, S. Grigorescu, I. N. Mihailescu, N. A. Vainos, J. Appl. Phys. **98**(7), 074312 (2005).
[17] Z. Y. Wu, J. H. Cai, G. Ni, Thin Solid Films **516,** 7318 (2008).
[18] N. Kavasoglu, A. S. Kavasoglu, Physica B **403,** 3159 (2008).
[19] F. Yakuphanoglu, S. Ilican, M. Caglar, Y. Caglar, J. Optoelectron. Adv. Mater. **9,** 2180 (2007).
[20] H. J. Fan, B. Fuhrmann, R. Scholz, C. Himcinschi, A. Berger, H. Leipner, A. Dadgar, A. Krost, S. Christiansen, U. Gosele, M. Zacharias, Nanotechnology **17,** S231 (2006).
[21] P. T. Hsieh, Y. C. Chen, K. S. Kao, M. S. Lee, C. C. Cheng, J. Eur. Ceram. Soc. **27,** 3815 (2007).
[22] T. Schuler, M. A. Aegerter, Thin solid films **351**, 125 (1999).
[23] S. Parmod, K. Manoj, R. M. Mehra, Solid State Communications **147**, 465 (2008).
[24] S. Mihaiu, L. Marta, M. Zaharescu , J. Eur. Ceram. Soc. **27**, 551 (2007).
[25 D. A. G. Bruggeman , Ann. Phys**. 24,** 636 **(**1935).
[26] K. Ip, G. T. Thaler, H. Yang, S. Y. Han, Y. Li, D. P. Norton, S. J. Pearton, S. Jang , F. Ren , Cryst. Growth **287,** 149 (2006).
[27] D. Mondelaers , G. Vanhoyland , H. Van Den Rul, J. D'Haen , M. K. Van Bael , J. Mullens, L. C. Van Poucke, J. Sol-Gel Sci. Techn. **26**, 523 (2003).
[28] C. Hariharan, Applied Catalysis. A: General **304,** 55 (2006).

*Corresponding author: smihaiu@chimfiz.icf.ro